JACS
JOURNAL OF THE AMERICAN CHEMICAL SOCIETY
Article
pubs.acs.org/JACS

Zn^{2+}-Ligation DNAzyme-Driven Enzymatic and Nonenzymatic Cascades for the Amplified Detection of DNA

Chun-Hua Lu,[†] Fuan Wang,[†] and Itamar Willner*

Institute of Chemistry and The Minerva Center for Complex Biohybrid Systems, The Hebrew University of Jerusalem, Jerusalem 91904, Israel

Supporting Information

ABSTRACT: A generic fluorescence sensing platform for analyzing DNA by the Zn^{2+}-dependent ligation DNAzyme as amplifying biocatalyst is presented. The platform is based on the target DNA induced ligation of two substrate subunits and the subsequent opening of a beacon hairpin probe by the ligated product. The strand displacement of the ligated product by the beacon hairpin is, however, of limited efficiency. Two strategies are implemented to overcome this limitation. By one method, a "helper" nucleic acid sequence is introduced into the system, and this hybridizes with the DNAzyme components and releases the ligated product for opening of the hairpin. By the second method, a nicking enzyme (Nt.BspQI) is added to the system, and this nicks the duplex between the beacon and ligated product while recycling the free ligation product. By combining the two coadded components ("helper" sequence and nicking enzyme), the sensitive detection of the analyte is demonstrated (detection limit, 20 pM). The enzyme-free amplified fluorescence detection of the target DNA is further presented by the Zn^{2+}-dependent ligation DNAzyme-driven activation of the Mg^{2+}-dependent DNAzyme. According to this method, the Mg^{2+}-dependent DNAzyme subunits displace the ligated product, and the resulting assembled DNAzyme cleaves a fluorophore/quencher-modified substrate to yield fluorescence. The method enabled the detection of the target DNA with a detection limit corresponding to 10 pM. The different sensing platforms are implemented to detect the Tay–Sachs genetic disorder mutant.

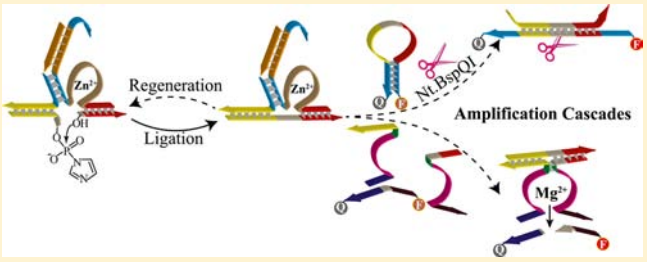

INTRODUCTION

Amplification of recognition events is a central element in analytical or bioanalytical sciences.[1] Different surface plasmonic effects, such as surface enhanced Raman spectroscopy (SERS), or coupling between localized plasmons of nanoparticles and surface plasmon waves, have been extensively used as physical phenomena for the amplified detection of sensing or biorecognition events.[2] Alternatively, the conjugation of catalysts or biocatalysts to recognition events provides a general route to develop amplified sensing platforms. Numerous sensor configurations for the amplified detection of immunocomplexes,[3] DNA,[4] or aptamer–substrate complexes[5] were reported using enzymes as amplifying labels. Similarly, metallic nanoparticles, e.g., Pt nanoparticles,[6] were used as electrocatalytic labels for the amplified detection of DNA or aptamer complexes.

The rapid progress in the design of catalytic nucleic acids (DNAzymes or ribozymes) introduced new catalytic tools for the development of amplified sensing assays,[7] for probing enzyme activities,[8] for analyzing DNA and aptamer–substrate complexes,[9] and for the detection of ions.[10] In these different amplified sensing systems, electrochemical[11] or optical (fluorescence, chemiluminescence)[12] signals were used as physical transduction stimuli. The amplified detection of DNA is of major importance in bioanalysis, and the ultrasensitive analysis of DNA has practical implications in medical diagnostics,[13] detection of environmental pollutants,[14] food quality control,[15] homeland security,[16] forensic applications,[17] and more. While the polymerase chain reaction (PCR) provides a versatile route to amplify DNA detection, the method is error-prone, requires special instrumentation, is time-consuming, and is difficult for adaptation for field tests. While the amplified detection of DNA using catalysts and biocatalysts was demonstrated,[4] the resulting sensitivities were limited. However, during the past few years, new paradigms for the ultrasensitive detection of DNA were introduced, using different catalytic constituents and a variety of amplification mechanisms. In these systems, the analyte may activate the autonomous synthesis of catalytic DNAzyme units[18] or stimulate the catalytic regeneration/recycling of the analyte itself.[19] Different enzyme-catalyzed machineries for the autonomous synthesis of DNAzyme units as a result of DNA recognition were reported. For example, the rolling circle amplification (RCA) process was used to synthesize long chains of the hemin/G-quadruplex horseradish peroxidase-mimicking DNAzyme, as a result of recognition of a target-DNA by a predesigned circle and the autonomous isothermal polymer-

Received: April 19, 2012
Published: May 21, 2012

dx.doi.org/10.1021/ja3037838 | J. Am. Chem. Soc. 2012, 134, 10651–10658

ization around the circular probe using polymerase/dNTPs.[20] Similarly, by the use of the predesigned DNA recognition track for the target DNA, the autonomous cyclic replication of the track DNA, and the displacement of the horseradish peroxidase-mimicking DNAzyme, using polymerase/dNTPs and a nicking enzyme as biocatalytic machineries were demonstrated.[20] The amplified detection of the analyte through the autonomous regeneration of the analyte was demonstrated by enzyme-catalyzed reactions that destroy the resulting probe/analyte duplex structure, while leaving the analyte strand intact for subsequent sensing cycles. Catalytic machineries that use polymerases,[21] Exo III,[22] endonucleases,[23] and nicking enzymes[24] were applied to regenerate the target DNA. Enzyme-free amplified detection of DNA has been accomplished by the autonomous generation of DNAzymes as labels.[25] The analyte-induced cross-opening of two nucleic acid hairpin structures, with the concomitant generation of polymeric micrometer-long DNAzyme wires, enabled the ultrasensitive detection of DNA. Also, predesigned DNA constructs trigger, upon sensing of the target DNA, the autonomous catabolic cleavage process, leading to the synthesis of DNAzyme units.[26] Recently, the Zn^{2+}-dependent ligation DNAzyme was applied as a catalytic label for the amplified detection of DNA by the autonomous synthesis of ligated reporter units that included the analyte sequence.[27] These reporter units stimulated the independent formation of ligation DNAzyme units that amplified the sensing events. Here we report on the application of the Zn^{2+}-dependent ligation DNAzyme[28] as catalyst for the amplified detection of DNA. We discuss the limitations of the DNAzyme as amplifying unit and present means to overcome these limitations by activating a variety of catalytic cascades. Besides the development of ultrasensitive DNA detection platforms, the results reveal new selection principles demonstrating the amplification of specific nucleic acid strands and their implementation as functional units for the activation of programmed catalytic cascades.

EXPERIMENTAL METHODS

Materials. 4-(2-Hydroxyethyl)piperazine-1-ethanesulfonic acid sodium salt (HEPES), sodium chloride, zinc chloride, magnesium chloride, imidazole, and 1-[3-(diethylamino)-propyl]-3-ethylcarbodiimide hydrochloride 98% (EDC·HCl) were purchased from Sigma-Aldrich Inc. The nicking enzyme Nt.BspQI was purchased from New England Biolabs Inc. (Beverly, MA, USA). All DNA oligonucleotides were purchased from Integrated DNA Technologies Inc. (Coralville, IA). Table S1 (Supporting Information) depicts the sequences of the oligonucleotides used in the study. The oligonucleotides were HPLC-purified. They were used as provided and diluted in 10 mM HEPES to give stock solutions of 100 μM. Ultrapure water from a NANOpure Diamond (Barnstead) source was used in all of the experiments.

Instrument. Fluorescence emission measurements were performed using a Cary Eclipse Device (Varian Inc.). The Cy3 dye was excited at a wavelength of 535 nm, and emission spectra were recorded at 565 nm. The Cy5 dye was excited at a wavelength of 630 nm, and emission spectra were recorded at 662 nm.

Detection of the Analyte DNA by Using the Zn^{2+}-Dependent Ligation DNAzyme. All the assays were prepared in 10 mM HEPES buffer (pH = 7.0) containing 100 mM NaCl and 10 mM $MgCl_2$. The working solution included 0.5 μM of the DNAzyme subunits (**4** and **5**), 1 μM of the substrate units (**2** and **3**), 0.5 μM of the hairpin probe (**8**), and 1 mM of Zn^{2+} ions. The optimization of the concentration of Zn^{2+} ions is shown in Figure S1 of the Supporting Information. Upon adding different concentrations of the target DNA, the mixture solution was allowed to incubate at 25 °C for 2 h. The total volume of each sample was 50 μL. After the ligation, the samples were diluted to 250 μL, and the fluorescence spectra were measured.

To improve the sensitivity of the system, the system was subjected to a secondary step after ligation. There are three ways to improve the sensitivity of the system: (i) The "helper" nucleic acid enlargement way. After ligation, 1 μM of the "helper" nucleic acid (**9**) was introduced into the system, and the mixture solutions were incubated for 1 h. Then the samples were diluted to 250 μL, and the fluorescence spectra were measured. (ii) The nicking enzymes amplification way. After ligation, 15 units of Nt.BspQI were introduced into the system, and the mixture solutions were incubated at 37 °C for 2 h. Then the samples were diluted to 250 μL, and the fluorescence spectra were measured. (iii) The combination of "helper" nucleic acid and nicking enzyme amplification way. After ligation, 1 μM of the "helper" nucleic acid (**9**) and 15 units of Nt.BspQI were introduced into the system, and the mixture solutions were incubated at 37 °C for 2 h. Then the samples were diluted to 250 μL, and the fluorescence spectra were measured.

The enzyme-free amplified detection of the analyte DNA by using the Zn^{2+}-dependent ligation DNAzyme and Mg^{2+}-dependent DNAzyme cascade was developed. The working solution included 0.5 μM of the Zn^{2+}-dependent DNAzyme subunits (**4** and **5**) and Mg^{2+}-dependent DNAzyme subunits (**12** and **13**), 1 μM of the substrate units (**2** and **3**), 1 μM of the DNAzyme substrate (**14**), and 1 mM of Zn^{2+} ions. Upon adding different concentrations of the target DNA, the mixture was allowed to incubate at 25 °C for 5 h. The sample was prepared in 10 mM HEPES buffer (pH = 7.0) containing 200 mM NaCl and 20 mM $MgCl_2$, and the total volume of each sample was 50 μL. After the ligation, the samples were diluted to 250 μL, and the fluorescence spectra were measured.

RESULTS AND DISCUSSION

Figure 1 outlines the principle to design the basic DNA-sensing platform that implements the Zn^{2+}-ligation DNAzyme. The DNAzyme sequence **1** binds the imidazole-modified substrate subunit **2** and the hydroxylated subunit **3**, leading in the presence of Zn^{2+} to the ligation of the 3′ and 5′ ends of the respective substrate subunits. We use the fact that the previously reported[28] ligation DNAzyme is stabilized by a hairpin domain (Figure 1A) and cleave, schematically, the hairpin sequence into two fragments: the subunit **4** includes a part of the DNAzyme sequence that binds the substrate subunit **2**; the second fragment **5** includes the second sequence of the ligation DNAzyme, domain **I**, that is extended by a hairpin domain (**II**). The resulting nucleic acid (**5**) binds the second substrate subunit, **3**. The added hairpin domain (**II**) is essential for the sensing platform, as its "stem" duplex region prohibits the formation of the DNAzyme nanostructure between the **4** and **5** subunits. The loop of the added hairpin (**II**) includes, however, the single-stranded domain that recognizes the triggering target DNA. Figure 1B outlines the basic sensing configuration for the analysis of a DNA target (**6**) that is recognized by the loop domain of the hairpin region **II**. In the presence of the analyte (**6**), the hairpin domain (**II**) opens,

dx.doi.org/10.1021/ja3037838 | J. Am. Chem. Soc. 2012, 134, 10651−10658

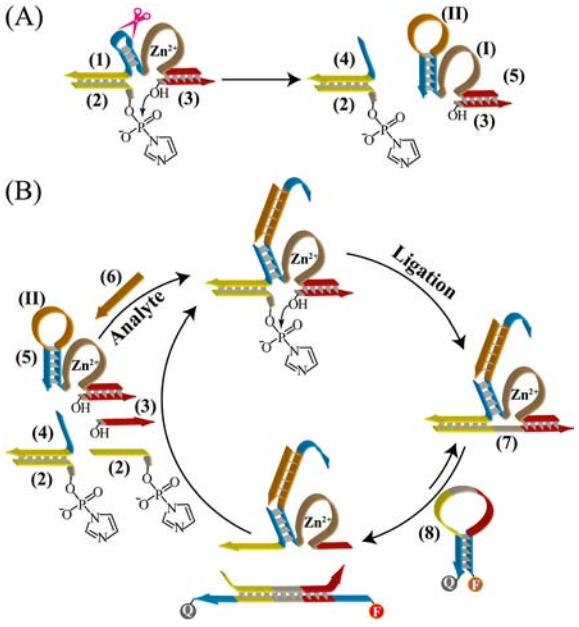

Figure 1. (A) Schematic separation of the Zn^{2+}-dependent ligation DNAzyme and its substrates into two subunits, where one subunit is functionalized with a hairpin structure that blocks the DNAzyme sequence and provides a recognition site for the target analyte DNA. (B) Amplified detection of the target DNA by the activation of the Zn^{2+}-dependent DNAzyme, recycling of the active ligation DNAzyme through the strand displacement of the ligated product by a fluorophore-quencher hairpin structure, and the fluorescence readout of the amplified detection cycle through the fluorescence of the open hairpin structure.

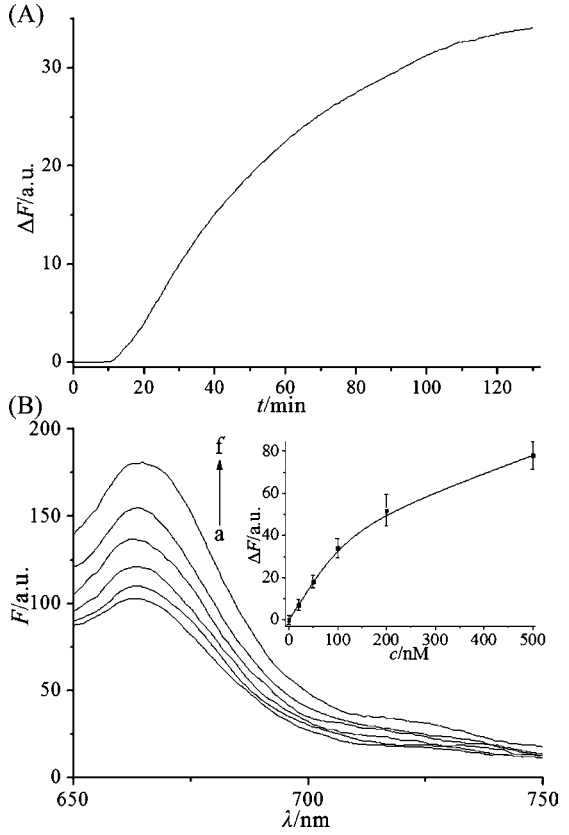

Figure 2. (A) Time-dependent fluorescence changes upon analyzing the target **6**, 100 nM, according to the scheme outlined in Figure 1B. (B) Fluorescence spectra generated by the system outlined in Figure 1B upon analyzing different concentrations of **6** for a fixed time interval of 2 h. Concentrations of target DNA correspond to (a) 0 nM; (b) 20 nM; (c) 50 nM; (d) 100 nM; (e) 200 nM; (f) 500 nM. Inset: Resulting calibration curve.

resulting in the self-assembly of the two DNAzyme/ and substrate subunits **4**/**2** and **5**/**3**. In the presence of Zn^{2+}, the DNAzyme is activated, resulting in the ligation of the subunits (**2** and **3**) to form the product **7**. To regenerate the DNAzyme as the amplifying label, and to optically follow the sensing event, the fluorophore/quencher-functionalized hairpin (**8**) is added to the system. The single-stranded loop region of **8** is complementary to the ligated product **7**. As the duplex between **7** and **8** is energetically favored with respect to the stability of the **7**/DNAzyme unit, strand displacement proceeds, resulting in the opening of **8** and the formation of the **7**/**8** duplex and the regeneration of the DNAzyme units. In the closed configuration of **8**, the fluorophore is quenched, while opening hairpin **8**, through the formation of the **7**/**8** duplex, leads to the activation of the fluorescence of the fluorophore, and this provides an optical readout signal for the ligation process. It should be noted that the loop domain (**II**) in the added hairpin constituent in **5** represents the variable sequence that is specific for target analytes, and it can be altered to fit any DNA target. In the present study we designed the loop region (II) of **5** to include the recognition sequence for one of the Tay–Sachs genetic disorder mutants. The disorder leading to the Tay–Sachs disease is caused by a deficiency of the enzyme hexosaminidase, which degrades GM2 ganglioside to GM3.[29] The disease is fatal in early childhood, and a survey reported that one in 30 Ashkenazi Jews is a carrier of the defective gene.[30]

Figure 2A shows the time-dependent fluorescence changes upon analyzing the target DNA according to Figure 1B. The fluorescence of the fluorophore intensified with time, and it levels off after ca. 2 h. Accordingly, the system was applied for analyzing different concentrations of the analyte **6**, by monitoring the resulting fluorescence after a fixed time interval of 2 h (Figure 2B). The fluorescence intensities increase upon elevation of the concentration of **6**, consistent with the enhanced opening of the probe hairpin **8**. From the derived calibration curve (Figure 2B, inset), the detection limit for analyzing the target DNA corresponds to 20 nM. Electrophoretic analysis of the mixture generated upon sensing of **6**, 0.5 μM, using the system shown in Figure 1B, and allowing the amplification process to proceed for 2 h, reveals, however, that the strand displacement process of the ligated product **7** is inefficient (Figure S2, Supporting Information). That is, the equilibrium content of **7**/**8**, as a result of the strand-displacement, is limited, resulting in the inhibition of the DNAzyme by the duplex formation with the ligated product **7**. Thus, the inefficient opening of the hairpin **8** by the ligated product leads to the relatively poor detection limits.

An approach to overcome the limitation of poor separation of the ligated product by the hairpin (**8**) is depicted in Figure 3A. According to this approach, we allow the ligation process to proceed for a fixed time interval and allow the system to reach its equilibrium composition, consisting of the ligated product linked to the Zn^{2+}-DNAzyme subunits and the **7**/**8** duplex composed of the ligated product and opened hairpin. This mixture is then subject to a "helper" nucleic acid (**9**) that facilitates the separation of the ligated product **7** from the Zn^{2+}-

dx.doi.org/10.1021/ja3037838 | J. Am. Chem. Soc. 2012, 134, 10651–10658

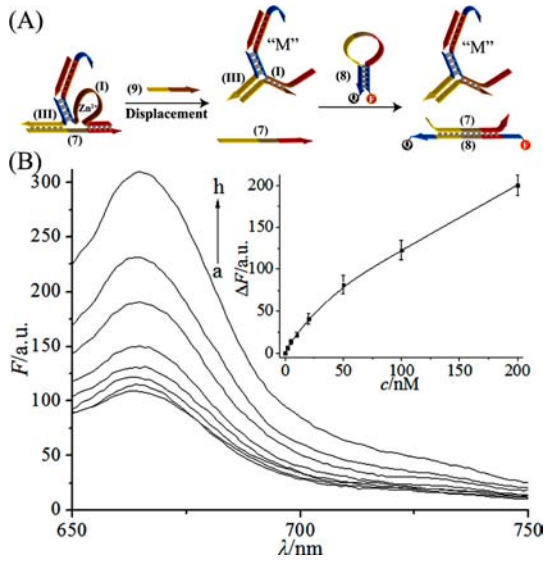

Figure 3. (A) Assisted separation of the Zn^{2+}-ligation DNAzyme/ligated product duplex by a "helper" unit that induces the strand displacement of the ligated product, and the opening of the fluorophore/quencher-labeled hairpin probe by the released ligated product. (B) Fluorescence spectra corresponding to the analysis of different concentrations of **6** using a two-step analysis process: In the first step the ligation process according to Figure 1B was conducted for 2 h followed by the second step, conducted for 1 h, where the ligated product **7** was displaced, resulting in the opening of hairpin **8**. Concentrations of target DNA correspond to (a) 0 nM; (b) 2 nM; (c) 5 nM; (d) 10 nM; (e) 20 nM; (f) 50 nM; (g) 100 nM; (h) 200 nM. Inset: Resulting calibration curve.

DNAzyme subunits. The "helper" nucleic acid (**9**) is complementary to the domains **I** and **III** of the two Zn^{2+}-ligation DNAzyme subunits. Due to the stability of the duplex structure between the helper and the DNAzyme units, strand displacement proceeds, resulting in the formation of structure "**M**" and the release of the ligated product that originally did not participate in the generation of the fluorescence signal. Naturally, this amplification path requires a two-step analysis, since the "helper" units can be added only after completion of the ligation process (otherwise the "helper" units prevent the assembly of the active DNAzyme units). Figure 3B shows the fluorescence spectra observed upon analyzing different concentrations of the analyte **6**, following the two-step analysis shown in Figure 3A. Figure 3B, inset, depicts the resulting calibration curve. The analyte **6** could be analyzed with a detection limit corresponding to 2 nM.

Another method to enhance the sensitivity of the sensing platform is depicted in Figure 4A. The mixture consisting of the duplex structure between the ligated product **7** and the DNAzyme subunits, and the duplex formed between **8** and the ligated product **7** is subjected to the nicking enzyme Nt.BspQI that cleaves the single strand domain of **8** in the duplex structure **7**/**8**. This results in the separation of the fluorophore-labeled fragment (**10**), the quencher-labeled nucleic acid fragment (**11**), and the regeneration of the ligated product (**7**) that further opens the hairpin structure (**8**). That is the nicking of the duplex structure **7**/**8** regenerated the ligated product, thus allowing the cyclic opening of hairpin **8** and the catalytic generation of the fluorophore labeled fragment (**10**). It should be noted, however, that the amplified detection of the analyte (**6**) through the ligation process and the nicking

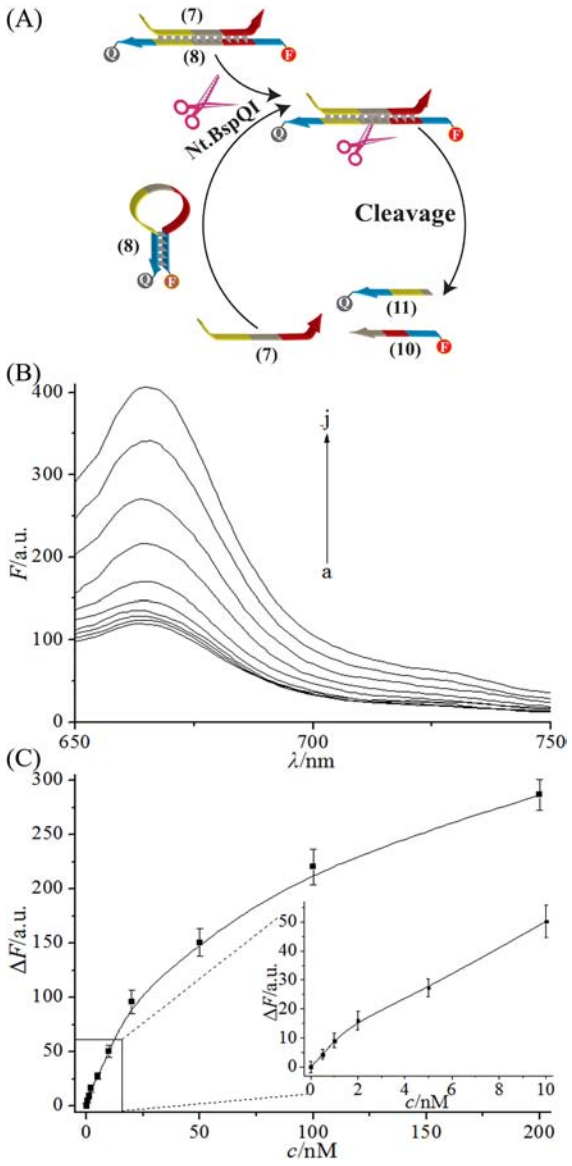

Figure 4. (A) Amplified detection of the target DNA (**6**) through the Zn^{2+}-ligation DNAzyme, separation of the ligated product **7** by hairpin **8**, and the catalytic nicking of the hairpin component in the duplex **7**/**8**, a process that recycles **7** for the autonomous cycle corresponding to the opening of hairpin **8**. (B) Fluorescence spectra corresponding to the analysis of different concentrations of the analyte **6** using the scheme outlined in Figure 1B that is coupled to the secondary amplification cycle that involves the nicking of the structure **7**/**8** according to Figure 4A. The analyses were performed using a two-step process: In step 1 (2 h), the ligation was conducted according to Figure 1B. In step 2 (2 h), amplified opening of **8** and nicking of the duplex **7**/**8** were conducted according to Figure 4A. Concentrations of target DNA correspond to (a) 0 nM; (b) 0.5 nM; (c) 1 nM; (d) 2 nM; (e) 5 nM; (f) 10 nM; (g) 20 nM; (h) 50 nM; (i) 100 nM; (j) 200 nM. (C) Resulting calibration curve using the secondary amplification cycle that includes the nicking enzyme.

enzyme amplification subcycle is performed in two steps. In the first step we allow the ligation process to proceed for a fixed time interval of 2 h, and then the system is treated with the mercaptoethanol, 1×10^{-5} M, for 20 min, and subsequently subjected to the nicking enzyme Nt.BspQI for a time interval of 2 h. This two-step analytical process is essential, since the imidazole-functionalized nucleic acid (**2**) reacts with cysteine

dx.doi.org/10.1021/ja3037838 | J. Am. Chem. Soc. 2012, 134, 10651−10658

residues of Nt.BspQI to yield the covalent attachment of the nucleic acid subunit to the nicking enzyme. This reaction leads to the deactivation of the nicking enzyme and thus perturbs its amplifying function. The two-step process preserves the content of **2** for the ligation process and allows the optimal amplification by the nicking enzyme. Figure 4B shows the fluorescence spectra generated by the system that includes the nicking enzyme upon analyzing different concentrations of the target DNA for a fixed time interval of 2 h (Figure S3, Supporting Information). As the concentrations of the target (**6**) are elevated, the resulting fluorescence is intensified, consistent with increased amounts of the cleaved off free fluorophore (**10**). Figure 4C shows the resulting calibration curve. This method enabled the sensing of the analyte **6** with a detection limit corresponding to 0.5 nM. Despite the 40-fold improvement of the detection limit by the nicking enzyme-stimulated regeneration of the ligation product, the sensitivity of the sensing platform remained unsatisfactory.

We, then, applied a combined two-step analysis scheme, where the "helper" units and the nicking enzyme Nt.BspQI act cooperatively in the secondary amplification step (Figure 5A). According to this scheme, the primary ligation process is conducted as the first step, and it is followed by the effective separation of the ligated product by the "helper" units, followed by the nicking enzyme-mediated regeneration of the ligated product. Figure 5B shows the fluorescence spectra generated by the system in the presence of variable concentrations of the analyte **6**. As the concentration of the analyte is higher, the fluorescence is intensified. These results are consistent with the higher content of ligated product as the concentration of **6** is elevated, the enhanced separation of the ligated product by the "helper" units, and the amplified generation of the fluorescent readout signal, formed by **10**, through the nicking enzyme-mediated regeneration of the ligated product. Figure 5C shows the derived calibration curve. This system enabled the detection of the analyte **6** with a detection limit that corresponded to 20 pM. The results demonstrate that the initial amplified detection scheme that involved the Zn^{2+}-ligation DNAzyme as amplifying catalyst could be improved by coupling a secondary amplification cycle that includes the "helper"-assisted separation of the ligated product and the nicking enzyme-mediated regeneration of the ligated product. While the resulting sensing platform reveals a satisfactory detection limit, it suffers from two limitations: (i) The sensing scheme is complex and involves a two-step analysis process. (ii) The system includes a nicking enzyme that increases the cost of the analysis and introduces aspects of enzyme stability and specific activity that affect the sensing platform.

To circumvent these difficulties, we decided to eliminate the need for a stable hairpin structure as the functional unit for the separation of the ligated product and as the fluorescence reporter of the ligation process. This is exemplified in Figure 6A with the design of an enzyme-free amplified detection of DNA that is driven by the Zn^{2+}-ligation DNAzyme that activates a secondary autonomous DNAzyme amplifying cascade. Upon interaction of the analyte **6** with the ligation DNAzyme fragments and their substrates, (**4**)/(**2**) and (**5**)/(**3**), in the presence of Zn^{2+} ions, ligation proceeds to yield the ligated product (**7**) that is hybridized with the Mg^{2+}-dependent DNAzyme subunits. The system includes, however, additional constituents **12** and **13**, that include the sequences corresponding to subunits of the Mg^{2+}-dependent DNAzyme, and a fluorophore/quencher-labeled strand **14** that acts as substrate

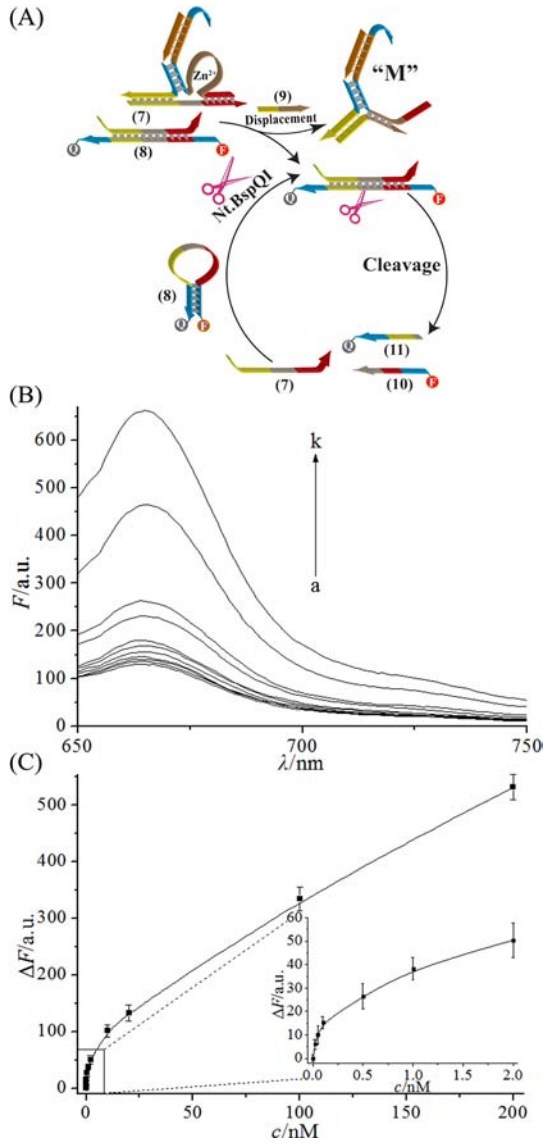

Figure 5. (A) Amplified detection of the target DNA (**6**), using the Zn^{2+}-ligation DNAzyme and a secondary amplification cycle combing the "helper" unit for separation of the ligated product and the nicking enzyme for the recycling of the ligated product for the autonomous opening of hairpin **8**. (B) Fluorescence spectra corresponding to the analysis of different concentrations of **6** according to the scheme shown in Figure 1B that is coupled to the secondary amplification cycle consisting of the "helper"/nicking enzyme components outlined in Figure 5A. The analyses are performed in a two-step process: Step 1 (2 h): ligation according to Figure 1B. Step 2 (2 h): secondary amplification cycle that includes the "helper"/nicking enzyme, according to Figure 5A. Concentrations of target DNA correspond to (a) 0 pM; (b) 20 pM; (c) 50 pM; (d) 100 pM; (e) 500 pM; (f) 1 nM; (g) 2 nM; (h) 10 nM; (i) 20 nM; (j) 100 nM; (k) 200 nM. (C) Resulting calibration curve.

for the Mg^{2+}-dependent DNAzyme. The subunits of the Mg^{2+}-dependent DNAzyme, **12** and **13**, include extended domains **IV** and **V**, which are complementary to the ligated product (**7**). Note, however, that the number of complementary bases between domain **V** and the respective region of the ligated product is higher than the number of complementary bases between **7** and subunit **5**. Thus, upon formation of the ligated product, the nucleic acid strands **12** and **13** induce a strand-displacement process, where **7** bridges the subunits **12** and **13**,

dx.doi.org/10.1021/ja3037838 | J. Am. Chem. Soc. 2012, 134, 10651−10658

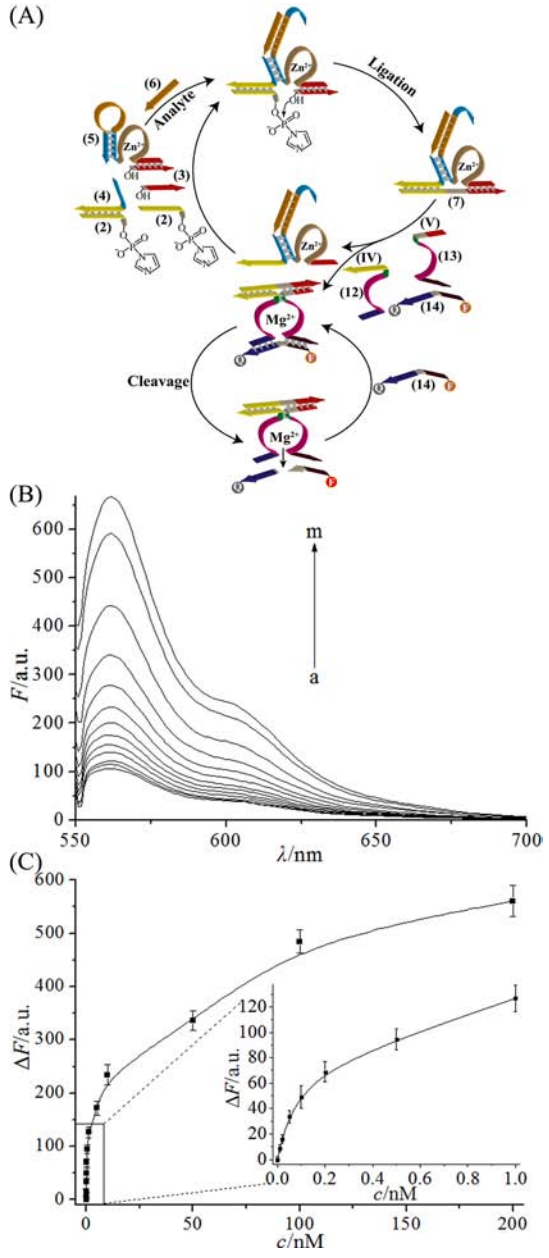

Figure 6. (A) Enzyme-free, amplified detection of DNA (**6**), using the Zn^{2+}-ligation DNAzyme coupled to the secondary displacement of the ligated product by the Mg^{2+}-dependent DNAzyme that cleaves the fluorophore/quencher-modified substrate (**14**). (B) Fluorescence spectra corresponding to the analysis of **6** according to the scheme outlined in Figure 6A recorded after a fixed time interval of 5 h. Concentrations of target DNA correspond to (a) 0 pM; (b) 10 pM; (c) 20 pM; (d) 50 pM; (e) 100 pM; (f) 200 pM; (g) 500 pM; (h) 1 nM; (i) 5 nM; (j) 10 nM; (k) 50 nM; (l) 100 nM; (m) 200 nM. (C) Resulting calibration curve.

and the resulting bridged nanostructure is further stabilized by hybridization with the fluorophore/quencher-modified substrate **14**. Therefore, the formation of the nanostructure **7**/**12**–**13**/**14** regenerates the ligation DNAzyme and generates the intact Mg^{2+}-dependent DNAzyme structure. In the presence of Mg^{2+} ions, the cleavage of the substrate proceeds, giving rise to the generation of fluorescence. The cyclic cleavage of the substrate by the Mg^{2+}-dependent DNAzyme provides a secondary amplification cycle. It should be noted that an analogous DNA-induced assembly of the Mg^{2+}-dependent DNAzyme subunits has been recently implemented to develop logic gate cascades.[31] The scheme shown in Figure 6A highlights several important amplification features: (i) The ligation DNAzyme provides the primary amplification cycle through the recognition of the analyte, **6**. (ii) The Mg^{2+}-dependent DNAzyme subunits provide the machinery to separate the ligated product, to regenerate the ligation DNAzyme, and to generate the Mg^{2+}-dependent DNAzyme that cleaves the substrate **14** and yields the readout signal for the sensing platform, and provides a secondary amplification cycle. (iii) The analytical scheme is enzyme-free and, thus, presents a robust sensing process that is cost-effective and is insensitive to protein–enzyme stabilities. Figure 6B shows the fluorescence spectra generated by different concentrations of the analyte (**6**), using the Mg^{2+}-dependent DNAzyme as the autonomous cascade amplification cycle. As the concentration of the analyte increases, the fluorescence intensities are higher, consistent with the formation of elevated amounts of the Mg^{2+}-dependent DNAzyme as the concentration of the analyte increases. Figure 6C depicts the resulting calibration curve for analyzing **6**. The analyte could be sensed with a detection limit corresponding to 10 pM. Table 1 summarizes the detection limits of different amplified DNA detection platforms. One may realize that the analytical platforms involving the target-induced replication of catalytic DNAzyme units reveal a ca. 10^3-fold enhanced sensitivity than the systems described in the present studies. On the other hand, the nicking enzyme-assisted amplification of the target DNA, presented in the present study, reveals comparable detection limits to other systems comprising enzymatic regeneration of the target analyte. Furthermore, the amplified detection of DNA by the Zn^{2+}- and Mg^{2+}-dependent DNAzyme cascade described in the present study reveals improved or comparable sensitivities to other DNAzyme- or metal nanoparticle-amplified DNA detection schemes.

The results demonstrate an attractive, highly sensitive, detection scheme for the Tay–Sachs mutant. For practical implications, the specificity of the sensing platform needs, however, to be confirmed. Figure 7, curve a, shows the time-dependent fluorescence changes upon analyzing the target Tay–Sachs mutant (**6**), 100 nM, according to the scheme outlined in Figure 6A. For comparison, curve b shows the time-dependent fluorescence changes upon analyzing the normal gene (**6a**). Evidently, a 4-fold lower fluorescence is observed, implying that the mutant can be discriminated from the normal gene. It should be noted that the substantially higher fluorescence signals observed in the presence of the Tay–Sachs mutant, as compared to the normal gene, enabled the clear fluorescence discrimination of the mutant, at a concentration of 1 nM, in the presence of a 100 nM background concentration of the normal gene.

CONCLUSIONS

In conclusion, the present study has introduced the Zn^{2+}-dependent ligation DNAzyme as an amplifying catalyst for DNA detection. The utilization of the ligated product as reporter unit for the sensing event is accompanied by advantages and inherent disadvantages. While the use of a ligated product as generator of the readout signal promises low background signals, the stability of the duplex resulting between the ligated product and the DNAzyme is always high, leading to inefficient separation of the ligated product and to low readout

dx.doi.org/10.1021/ja3037838 | J. Am. Chem. Soc. 2012, 134, 10651–10658

Table 1. Different Amplified DNA Detection Platforms

	amplification method	detection limit	detection signal	ref
enzymatic amplification	electrocatalytic enzyme label	1×10^{-10} M	electrochemical	4d
	exo III regeneration of analyte	5×10^{-12} M	fluorescence	22c
	endonuclease regeneration of analyte	1×10^{-12} M	electrochemical	23b
	nicking enzyme-assisted amplification	2×10^{-11} M	fluorescence	present study
enzyme replication machinery	polymerization/nicking DNA machinery	1×10^{-14} M	colorimetric/luminescence	18
	rolling circle amplification	1×10^{-14} M	colorimetric/luminescence	20b
DNAzyme	HRP-mimicking DNAzyme	1×10^{-10} M	colorimetric/luminescence	9e
	Mg^{2+}-dependent DNAzyme	1×10^{-12} M	fluorescence	26
	Zn^{2+}-dependent DNAzyme	1×10^{-11} M	fluorescence	27
	Zn^{2+}- and Mg^{2+}- dependent DNAzyme cascade	1×10^{-11} M	fluorescence	present study
metal nanoparticles	aggregation of nanoparticles	5×10^{-9} M	colorimetric	32
	electrochemical stripping	2×10^{-14} M	electrochemical	6a
	electrocatalytic reduction of H_2O_2 by Pt nanoparticles	1×10^{-11} M	electrochemical	6b
	catalytic Pt nanoparticles generation of chemiluminescence	1×10^{-11} M	luminescence	1b

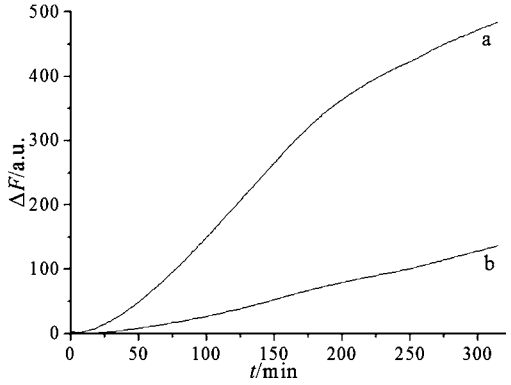

Figure 7. Time-dependent fluorescence changes upon analyzing: (a) the Tay–Sachs mutant (**6**), 100 nM, and (b) the normal gene (**6a**), 100 nM, according to Figure 6A.

signals (low sensitivity). These limitations can be resolved, however, by coupling secondary amplification cycles that assist the separation of the ligated product and/or activate secondary catalytic cascades for the recycling of the released ligated product. In the present study, we demonstrated several methods to improve the primary Zn^{2+} ligation DNAzyme-driven amplified detection of the analyte DNA. By introducing a "helper" nucleic acid to displace the ligated nucleic acid or by implementing a nicking enzyme as catalyst for the recycling of the ligation product, the fluorescence readout signal was intensified. By combining the "helper" units and the nicking enzyme as an integrated amplifying mechanism, the detection limit for analyzing the target DNA corresponded to 20 pM. The sensing platform involving the ligation DNAzyme and the coupled "helper"/nicking enzyme amplifying cascade suffered, however, from basic difficulties associated with the complexity of the system (two-step procedure) and the stability/activity limitations of the nicking enzyme. To resolve these problems, we implemented an alternative approach, where the analyte drives the Zn^{2+}-ligation DNAzyme that synthesizes as ligated product, that assembled the Mg^{2+}-dependent DNAzyme. This resulted in the Mg^{2+}-dependent DNAzyme cascade as the second amplification cycle. One may use the latter approach to analyze any DNA target by the appropriate alternation of the single-stranded domain associated with the hairpin structure of **5**. Besides the analytical implications of the system, we demonstrate an enzyme-free replication reaction that may provide a simple model for an evolutionary process.

■ ASSOCIATED CONTENT

Ⓢ Supporting Information

Sequences of the DNA; experimental procedure for imidazole modification of DNA; and denatured and native electrophoresis gel characterization. This material is available free of charge via the Internet at http://pubs.acs.org.

■ AUTHOR INFORMATION

Corresponding Author

willnea@vms.huji.ac.il

Author Contributions

†These authors contributed equally.

Notes

The authors declare no competing financial interest.

■ ACKNOWLEDGMENTS

This research was supported by The Israel Science Foundation.

■ REFERENCES

(1) (a) Wang, J. *Small* **2005**, *1*, 1036–1043. (b) Gill, R.; Polsky, R.; Willner, I. *Small* **2006**, *2*, 1037–1041. (c) Scrimin, P.; Prins, L. J. *Chem. Soc. Rev.* **2011**, *40*, 4488–4505.

(2) (a) Jeanmaire, D. L.; Van Duyne, R. P. *J. Electroanal. Chem.* **1977**, *84*, 1–20. (b) Lyon, L. A.; Musick, M. D.; Natan, M. J. *Anal. Chem.* **1998**, *70*, 5177–5183. (c) He, L.; Musick, M. D.; Nicewarner, S. R.; Sallinas, F. G.; Benkovic, S. J.; Natan, M. J.; Keating, C. D. *J. Am. Chem. Soc.* **2000**, *122*, 9071–9077. (d) Liu, Y. C.; Wang, C. C. *J. Phys. Chem. B* **2005**, *109*, 5779–5782. (e) Wang, Y. L.; Wei, H.; Li, B. L.; Ren, W.; Guo, S. J.; Dong, S. J.; Wang, E. K. *Chem. Commun.* **2007**, 5220–5222. (f) Riskin, M.; Tel-Vered, R.; Lioubashevski, O.; Willner, I. *J. Am. Chem. Soc.* **2009**, *131*, 7368–7378. (g) Wang, Y. L.; Irudayaraj, J. *Chem. Commun.* **2011**, *47*, 4394–4396.

(3) (a) Ivnitski, D.; Rishpon, J. *Biosens. Bioelectron.* **1996**, *11*, 409–417. (b) Rishpon, J.; Ivnitski, D. *Biosens. Bioelectron.* **1997**, *12*, 195–204.

(4) (a) Caruana, D. J.; Heller, A. *J. Am. Chem. Soc.* **1999**, *121*, 769–774. (b) Patolsky, F.; Lichtenstein, A.; Willner, I. *Nat. Biotechnol.* **2001**, *19*, 253–257. (c) Patolsky, F.; Weizmann, Y.; Willner, I. *J. Am. Chem. Soc.* **2002**, *124*, 770–772. (d) Zhang, Y.; Kim, H.-H.; Heller, A. *Anal. Chem.* **2003**, *75*, 3267–3269. (e) Li, J. W. J.; Chu, Y. Z.; Lee, B. Y.-H.; Xie, X. L. S. *Nucleic Acids Res.* **2008**, *36*, e36. (f) Ferapontova, E. E.; Hansen, M. N.; Saunders, A. M.; Shipovskov, S.; Sutherlandc, D. S.; Gothelf, K. V. *Chem. Commun.* **2010**, *46*, 1836–1838.

(5) (a) Zhu, C. F.; Wen, Y. Q.; Li, D.; Wang, L. H.; Song, S. P.; Fan, C. H.; Willner, I. *Chem.—Eur. J.* **2009**, *15*, 11898–11903. (b) Wen, Y. L.; Pei, H.; Wan, Y.; Su, Y.; Huang, Q.; Song, S. P.; Fan, C. H. *Anal.*

Chem. **2011**, *83*, 7418−7423. (c) Zhu, C. L.; Lu, C. H.; Song, X. Y.; Yang, H. H.; Wang, X. R. *J. Am. Chem. Soc.* **2011**, *133*, 1278−1281.
(6) (a) Wang, J.; Xu, D.; Polsky, R. *J. Am. Chem. Soc.* **2002**, *124*, 4208−4209. (b) Polsky, R.; Gill, R.; Kaganovsky, L.; Willner, I. *Anal. Chem.* **2006**, *78*, 2268−2271.
(7) (a) Willner, I.; Shlyahovsky, B.; Zayats, M.; Willner, B. *Chem. Soc. Rev.* **2008**, *37*, 1153−1165. (b) Liu, J.; Cao, Z.; Lu, Y. *Chem. Rev.* **2009**, *109*, 1948−1998. (c) Kolpashchikov, D. M. *Chem. Rev.* **2010**, *110*, 4709−4723. (d) Gerasimova, Y. V.; Kolpashchikov, D. M. *Chem. Biol.* **2010**, *17*, 104−106.
(8) (a) Niazov, T.; Pavlov, V.; Xiao, Y.; Gill, R.; Willner, I. *Nano Lett.* **2004**, *4*, 1683−1687. (b) Shlyahovsky, B.; Li, D.; Katz, E.; Willner, I. *Biosens. Bioelectron.* **2007**, *22*, 2570−2576. (c) Li, W.; Liu, Z. L.; Lin, H.; Nie, Z.; Chen, J. H.; Xu, X. H.; Yao, S. Z. *Anal. Chem.* **2010**, *82*, 1935−1941. (d) Li, Y.; Li, X.; Ji, X.; Li, X. *Biosens. Bioelectron.* **2011**, *26*, 4095−4098.
(9) (a) Tian, Y.; Mao, C. *Talanta* **2005**, *67*, 532−537. (b) Li, D.; Shlyahovsky, B.; Elbaz, J.; Willner, I. *J. Am. Chem. Soc.* **2007**, *129*, 5804−5805. (c) Teller, C.; Shimron, S.; Willner, I. *Anal. Chem.* **2009**, *81*, 9114−9119. (d) Ali, M. M.; Li, Y. *Angew. Chem., Int. Ed.* **2009**, *48*, 3512−3515. (e) Elbaz, J.; Moshe, M.; Shlyahovsky, B.; Willner, I. *Chem.—Eur. J.* **2009**, *15*, 3411−3418.
(10) (a) Liu, J.; Lu, Y. *J. Am. Chem. Soc.* **2003**, *125*, 6642−6643. (b) Liu, J.; Lu, Y. *J. Am. Chem. Soc.* **2004**, *126*, 12298−12305. (c) Liu, J.; Lu, Y. *J. Am. Chem. Soc.* **2007**, *129*, 9838−9839. (d) Li, D.; Wieckowska, A.; Willner, I. *Angew. Chem., Int. Ed.* **2008**, *47*, 3927−3931. (e) Elbaz, J.; Shlyahovsky, B.; Willner, I. *Chem. Commun.* **2008**, 1569−1571.
(11) (a) Xiao, Y.; Rowe, A. A.; Plaxco, K. W. *J. Am. Chem. Soc.* **2007**, *129*, 262−263. (b) Pelossof, G.; Tel-Vered, R.; Elbaz, J.; Willner, I. *Anal. Chem.* **2010**, *82*, 4396−4402.
(12) (a) Lu, C. H.; Li, J.; Liu, J. J.; Yang, H. H.; Chen, X.; Chen, G. N. *Chem.—Eur. J.* **2010**, *16*, 4889−4894. (b) Liu, X.; Freeman, R.; Golub, E.; Willner, I. *ACS Nano* **2011**, *5*, 7648−7655. (c) Freeman, R.; Liu, X.; Willner, I. *J. Am. Chem. Soc.* **2011**, *133*, 11597−11604. (d) Zheng, A. X.; Li, J.; Wang, J. R.; Song, X. R.; Chen, G. N.; Yang, H. H. *Chem. Commun.* **2012**, *48*, 3112−3114.
(13) (a) Botezatu, I.; Serdyuk, O.; Potapova, G.; Shelepov, V.; Alechina, R.; Molyaka, Y.; Ananev, V.; Bazin, I.; Garin, A.; Narimanov, M.; Knysh, V.; Melkonyan, H.; Umansky, S.; Lichtenstein, A. *Clin. Chem.* **2000**, *46*, 1078−1084. (b) Lu, C. H.; Yang, H. H.; Zhu, C. L.; Chen, X.; Chen, G. N. *Angew. Chem., Int. Ed.* **2009**, *48*, 4785−4787. (c) Brady, T.; Roth, S. L.; Malani, N.; Wang, G. P.; Berry, C. C.; Leboulch, P.; Hacein-Bey-Abina, S.; Cavazzana-Calvo, M.; Papapetrou, E. P.; Sadelain, M.; Savilahti, H.; Bushman, F. D. *Nucleic Acids Res.* **2011**, *39*, e72. (d) Lu, C. H.; Zhu, C. L.; Li, J.; Liu, J. J.; Chen, X.; Yang, H. H. *Chem. Commun.* **2010**, *46*, 3116−3118.
(14) Bagni, G.; Osella, D.; Sturchio, E.; Mascini, M. *Anal. Chim. Acta* **2006**, *573*−*574*, 81−89.
(15) Patel, P. D. *Trends Anal. Chem.* **2002**, *21*, 96−115.
(16) Call, D. R. *Crit. Rev. Microbiol.* **2005**, *31*, 91−99.
(17) Bond, J. W. J. *Forensic Sci.* **2007**, *52*, 128−136.
(18) Weizmann, Y.; Beissenhirtz, M. K.; Cheglakov, Z.; Nowarski, R.; Kotler, M.; Willner, I. *Angew. Chem., Int. Ed.* **2006**, *45*, 7384−7388.
(19) (a) Lu, C. H.; Li, J.; Lin, M. H.; Wang, Y. W.; Yang, H. H.; Chen, X.; Chen, G. N. *Angew. Chem., Int. Ed.* **2010**, *49*, 8454−8457. (b) Chen, Y.; Jiang, B. Y.; Xiang, Y.; Chai, Y. Q.; Yuan, R. *Chem. Commun.* **2011**, *47*, 12798−12800. (c) Zou, B. J.; Ma, Y. J.; Wu, H. P.; Zhou, G. H. *Angew. Chem., Int. Ed.* **2011**, *50*, 7395−7398. (d) Liu, X.; Freeman, R.; Willner, I. *Chem.—Eur. J.* **2012**, *18*, 2207−2211.
(20) (a) Tian, Y.; He, Y.; Mao, C. *ChemBioChem* **2006**, *7*, 1862−1864. (b) Cheglakov, Z.; Weizmann, Y.; Basnar, B.; Willner, I. *Org. Biomol. Chem.* **2007**, *5*, 223−225.
(21) (a) Guo, Q. P.; Yang, X. H.; Wang, K. M.; Tan, W. H.; Li, W.; Tang, H. X.; Li, H. M. *Nucleic Acids Res.* **2009**, *37*, e20. (b) Wu, Z, S.; Zhang, S. B.; Zhou, H.; Shen, G. L.; Yu, R. Q. *Anal. Chem.* **2010**, *82*, 2221−2227. (c) He, J. L.; Wu, Z. S.; Zhou, H.; Wang, H. Q.; Jiang, J. H.; Shen, G. L.; Yu, R. Q. *Anal. Chem.* **2010**, *82*, 1358−1364.
(22) (a) Zuo, X.; Xia, F.; Xiao, Y.; Plaxco, K. W. *J. Am. Chem. Soc.* **2010**, *132*, 1816−1818. (b) Freeman, R.; Liu, X.; Willner, I. *Nano Lett.* **2011**, *11*, 4456−4461. (c) Liu, X.; Aizen, R.; Freeman, R.; Yehezkeli, O.; Willner, I. *ACS Nano* **2012**, *6*, 3553−3563.
(23) (a) Chen, J. H.; Zhang, J.; Yang, H. H.; Fu, F. F.; Chen, G. N. *Biosens. Bioelectron.* **2010**, *26*, 144−148. (b) Wang, Q.; Yang, L. J.; Yang, X. H.; Wang, K. M.; He, L. L.; Zhu, J. Q.; Su, T. Y. *Chem. Commun.* **2012**, *48*, 2982−2984.
(24) (a) Xu, W.; Xue, X. J.; Li, T. H.; Zeng, H. Q.; Liu, X. G. *Angew. Chem., Int. Ed.* **2009**, *48*, 6849−6852. (b) Connolly, A. R.; Trau, M. *Angew. Chem., Int. Ed.* **2010**, *49*, 2720−2723.
(25) (a) Wang, F.; Elbaz, J.; Orbach, R.; Magen, N.; Willner, I. *J. Am. Chem. Soc.* **2011**, *133*, 17149−17151. (b) Shimron, S.; Wang, F.; Orbach, R.; Willner, I. *Anal. Chem.* **2012**, *84*, 1042−1048.
(26) Wang, F.; Elbaz, J.; Teller, C.; Willner, I. *Angew. Chem., Int. Ed.* **2011**, *50*, 295−299.
(27) Wang, F.; Elbaz, J.; Willner, I. *J. Am. Chem. Soc.* **2012**, *134*, 5504−5507.
(28) Cuenoud, B.; Szostak, J. W. *Nature* **1995**, *375*, 611−614.
(29) Gravel, R. A.; Clarke, J. T. R.; Kaback, M. M.; Mahuran, D.; Sandhoff, K.; Suzuki, K. In The Metabolic and Molecular Bases of Inherited Diseases; Scriver, C. R., Beaudet, A. L., Sly, W. S., Valle, D., Eds.; McGraw-Hill: New York, 1995; Vol. *2*, pp 2839−2879.
(30) Myerowitz, R.; Costigan, F. C. *J. Biol. Chem.* **1988**, *263*, 18587−18589.
(31) Elbaz, J.; Lioubashevski, O.; Wang, F.; Remacle, F.; Levine, R. D.; Willner, I. *Nat. Nanotechnol.* **2010**, *5*, 417−422.
(32) Elghanian, R.; Storhoff, J. J.; Mucic, R. C.; Letsinger, R. L.; Mirkin, C. A. *Science* **1997**, *277*, 1078−1081.